

NUMERICAL INVESTIGATION OF THE SEISMIC RESPONSE OF PRECAST BUILDINGS WITH INTEGRATED RC CLADDING WALLS

Ioannis Kalyviotis¹, Ioannis Psycharis²

¹ National Technical University of Athens
9 Heroon Polytechniou str., Zografou, Greece
e-mail: ikalyvio@central.ntua.gr

² National Technical University of Athens
9 Heroon Polytechniou str., Zografou, Greece
e-mail: ipsych@central.ntua.gr

Keywords: Precast buildings; Cladding walls; Fixed connections; Inelastic response; Precast walls.

Abstract. *Recent earthquakes have dramatically shown the importance of cladding connections on the seismic response of precast buildings. In the present work, a numerical investigation on the behaviour of precast structures with RC panel walls with ‘fixed’ connections is reported. Simplified structural calculations and numerical analyses show that the seismic forces induced to the connections of the panels can be quite large. An extensive numerical and experimental program has been performed at the Laboratory for Earthquake Engineering of the National Technical University of Athens, Greece, within the framework of the FP7 European project SAFECLADDING, for the investigation of the behaviour of integrated connections and their effect on the overall structural response. In the numerical analyses presented herein, the behaviour of the panel-beam connections was modeled with inelastic rotational springs which were calibrated against the experimental data. The results show that the roof diaphragm has a profound effect on the way the forces are transmitted to the structural members and on the forces induced to the connections. For typical ground motions compatible with the code requirements, the inelastic response is generally restricted to the columns, while the panels behave practically elastically.*

1 INTRODUCTION

In common design practice of precast structures, RC cladding panels are not designed to contribute to the structure's lateral stiffness but are connected to the structure with fastening devices dimensioned to bear the panels' self-weight, wind loads and seismic loads corresponding to the panels' mass only. However, the behaviour of cladding wall systems in recent strong earthquakes, v.i.z. Gölcük, Turkey (1999); Düzce, Turkey (1999); L'Aquila, Italy (2009); Lorca, Spain (2010); Emilia, Italy (2012), dramatically showed that simple connections typically applied in practice are insufficient to resist the large forces induced to them during strong ground shaking, resulting to severe damage to the connections and collapse of the panels.

New innovative panel-to-structure connections and novel design approaches for a correct conception and dimensioning of the fastening system to guarantee good seismic performance of the structure have been investigated within the FP7 European project "SAFECLADDING: Improved fastening systems of cladding wall panels of precast buildings in seismic zones", GA No. 314122. Part of this investigation concerned fixed panel connections, referred as "integrated", which are designed to resist the large seismic forces that develop in them since the panels contribute to the lateral load resisting system of the structure. To this end, experimental and analytical investigations on the behavior of fixed connections and their effect on the overall response of the structure were performed at the Laboratory for Earthquake Engineering of the National Technical University of Athens (NTUA), Greece [10].

In the integrated systems, the panel connections are based on a hyperstatic arrangement of the fixed supports of each panel. Typically, vertical panels are used connected to the beams at four points (Figure 1a) or at three points (Figure 1b). Horizontal panel arrangements could also be used, however they are not recommended as they transfer large forces to the columns to which they are connected. For this reason, horizontal panels are not examined in this paper.

Several mechanisms can be used to materialize fixed panel-to-beam connections, as simple connections made of protruding bars ('rebar' connections – Figure 2) or more sophisticated connections made of industrially produced bolted shoes. The analyses presented herein are based on connections of the first type.

Figure 2 shows a panel of height up to the zero-moment point (shear length, ℓ_s), which is equal to one half of the total height in case of Figure 1a, and equal to the full height in case of Figure 1b. The connecting bars provide the tensile strength in the tension zone, while concrete provides the resistance in the compression zone.

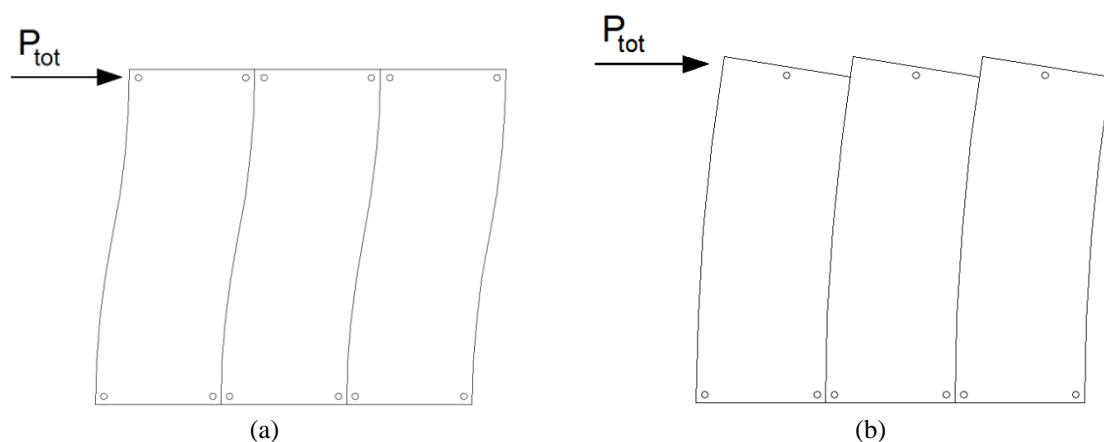


Figure 1. Arrangement of vertical panels with: (a) four connections; (b) three connections.

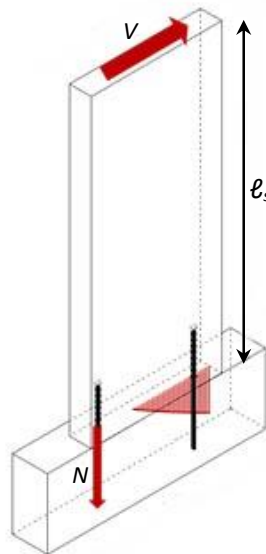


Figure 2. ‘Rebar’ connections: resisting mechanism at the panel-to-beam joint under seismic loading.

2 NUMERICAL MODELLING OF PANELS

2.1 General considerations

The overall lateral response of precast panels with integrated connections to lateral loading consists of the deformation of the panel itself and the response of the connection under tension. It is not easy to model this response numerically, since the latter involves tensile yielding of the bars and local debonding. For this reason, a simplified model is proposed, consisting of linear elements and nonlinear springs, capable to capture the overall response of the panel and the connections. In this model (Figure 3), the panel is modelled with 5 elastic beam elements while the panel-to-beam connections are modelled with hinges.

The panel behaviour is captured by the vertical beam element placed at the centerline of the panel and four horizontal elements are used to materialize the width of the panel and the eccentric connections with the beams. The inelastic response of the connections is modelled with inelastic rotational springs placed at the ends of the vertical beam element, the properties of which (moment – rotation law) are determined from an independent finite element analysis, as explained in the ensuing. Due to the opening of the panel-beam joint, zero-length nonlinear springs are used, since the overall nonlinear behaviour at the joint corresponds to a plastic hinge of zero length. In the out-of-plane direction, these springs behave elastically.

In Figure 3, the modelling of panels with four connections is shown. In case of panels with three connections, the same model can be used but with zero stiffness assigned to the top ‘zero-length spring’, in order to take under consideration that the panels are free to rotate at their top.

2.2 Moment – rotation law of the panel connections

As mentioned above, the Lumped Plasticity model is considered at the ends of the panels, where the overall inelastic behaviour at the panel-beam joint is modelled with zero-length springs. For the determination of the moment – rotation law that governs the behaviour of these springs, a special finite element analysis was performed using SAP 2000 [2].

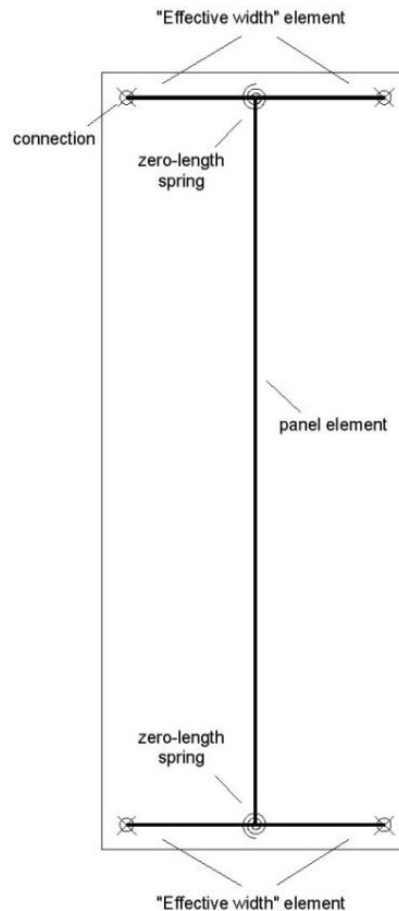


Figure 3. Numerical model of panel with four connections. In case of panel with three connections, the stiffness of the top 'zero-length spring' is set to zero.

Analyses were performed for panels with four and three connections. In the former case, the top beam was also included in the model (Figure 4a); in the latter, the panel was free at its top (Figure 4b). Both the panel and the beams were modelled with shell elements, while the connection bars were modelled with beam elements. In order to account for the possible debonding of the connection bars from the surrounding concrete, the nodes of the rebars were not connected directly to the corresponding nodes of the shell elements (modelling the panel or the beam), but through nonlinear springs, the behaviour of which was elastic – perfectly plastic. Thus, the 'bond' springs were yielding when the bond strength was reached, allowing local loss of the bonding along the bars. In order to capture well the local debonding, a quite dense mesh was applied around the rebars (max node distance was 20 mm). The joint between the panel and the beam was modelled with tensionless springs (gap elements). Representative results are shown in Figure 5.

The behaviour of the connections predicted by the numerical model was calibrated against the results of experiments conducted at NTUA concerning this type of connection. To this end, numerical models representing the test specimens (panels of height 2.65 m and length 1.50 m connected to the beam at their base and free at their top – Figure 2) were used and the derived capacity curves were compared with the experimental results for monotonic and cyclic loading. In this way, the appropriate properties of the springs modelling the bond between the connection bars and the concrete and the parameters of the contact springs were determined.

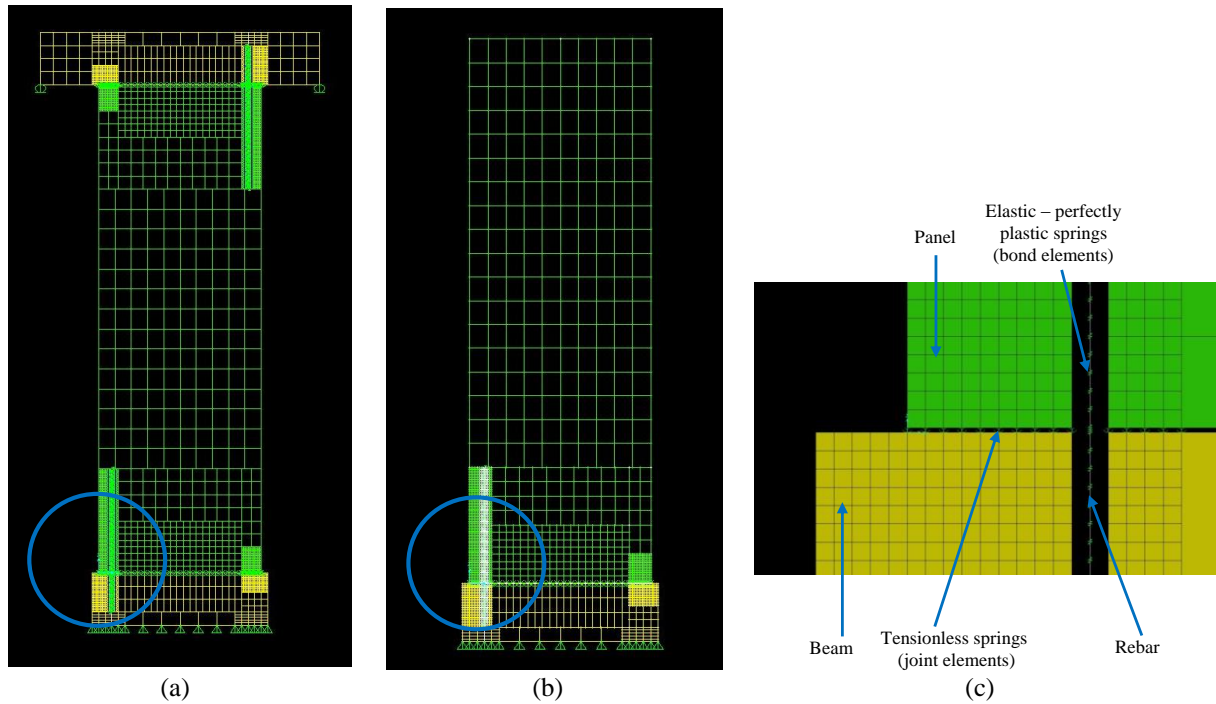


Figure 4. Model used for the analysis of the inelastic behaviour of panel-beam connections: (a) panels with four-point connections; (b) panels with three-point connections; (c) detail of connection.

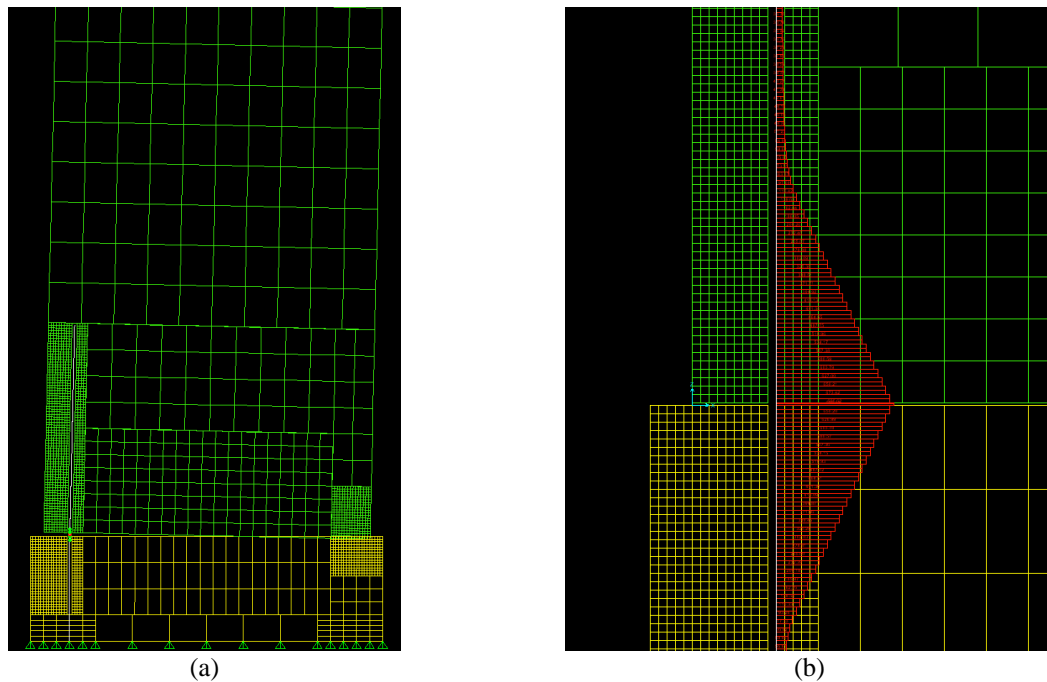


Figure 5. Representative numerical results: (a) deformed shape; (b) axial force induced to the connection bar at the final step of the analysis.

A comparison of the numerical results with the experimental data for the finally selected parameters is shown in Figure 6 for connections made of 1Ø25 rebars, in which the horizontal force at the top of the panel versus the top displacement of the panel is plotted. It can be observed that the numerical behaviour captures accurately the initial stiffness and the post yield response, but the yield force is somehow overestimated.

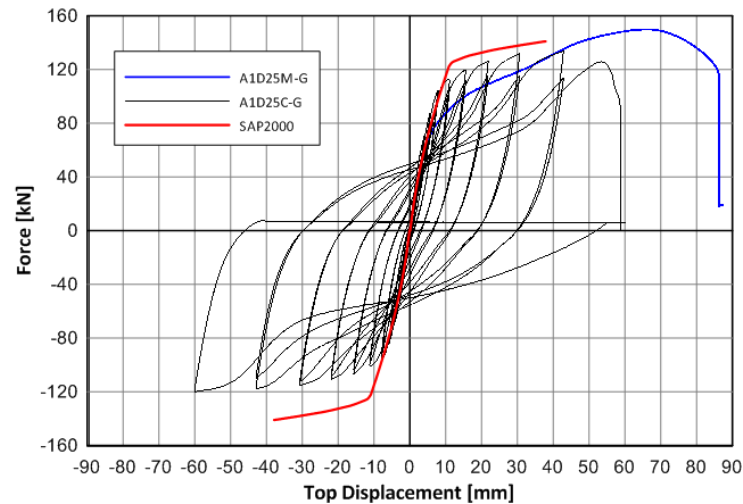


Figure 6. Comparison of the numerically predicted overall response (red line) of a panel with two bottom connections made of 1Ø25 bars with experimental data for monotonic (blue line) and cyclic (black line) excitation.

3 CASE STUDY

As a case study, a single-storey industrial building of dimensions: length 60 m, width 40 m and height 7.5 m (Figure 7) was considered. The roof consisted either of Y shape precast elements or double-tee elements. In the former case, the roof elements were connected at a single point with the beams (Figure 8a) and were not connected to each other; thus, there was small diaphragmatic action in the roof (denoted as ‘null diaphragm’). In the latter case, two configurations were examined: double-tee’s not connected to each other (denoted as ‘deformable diaphragm’ – Figure 8b) or double-tee’s connected to each other (denoted as ‘rigid diaphragm’ – Figure 8c).

The columns and the beams were of orthogonal cross section of dimensions 600 mm × 600 mm and 800 mm × 800 mm, respectively. Vertical panels of cross section 2500 mm × 200 mm were placed at all external sides, covering the full perimeter and the full height of the building. Analyses were performed for panels with three connections and for panels with four connections. The connections were made of vertical rebars of grade B500C and varying diameter (Table 1) and concrete grade C45/55. The building was designed according to EC2 [3] and EC8 [4].

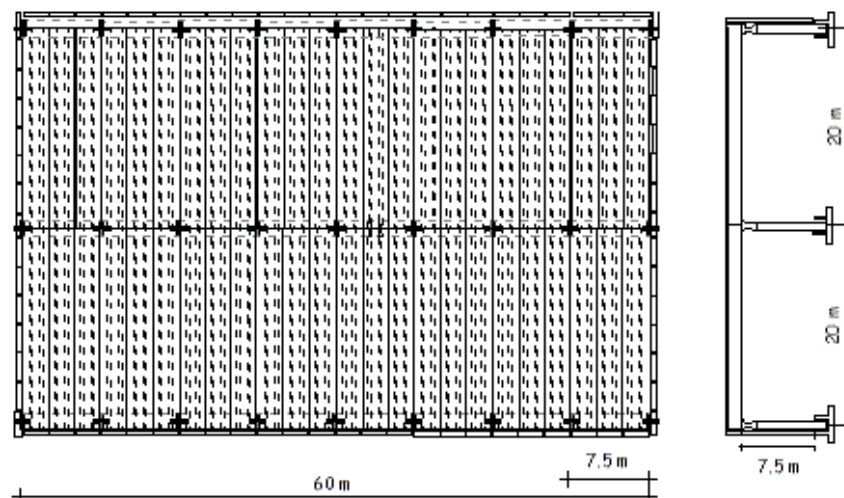


Figure 7. Plan view and cross section of the building considered.

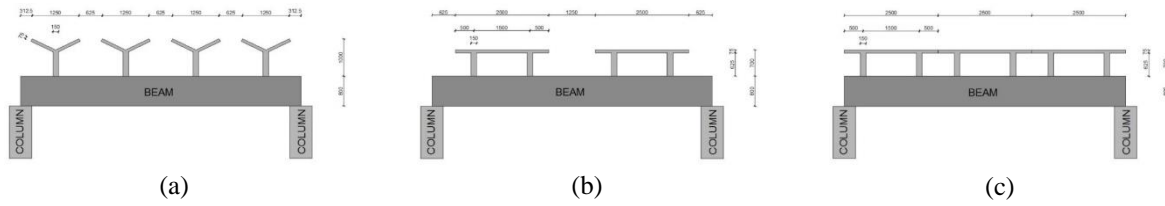


Figure 8. Roof Configurations: (a) null diaphragm; (b) deformable diaphragm; (c) rigid diaphragm.

Panel in X direction		Panel in Y direction	
4-point	3-point	4-point	3-point
1Ø25	2Ø25	1Ø28	2Ø28

Table 1. Rebars of the connections considered.

Property	Beam	Roof	Panel
Young's modulus [GPa]	36.0	36.0	36.0
Shear modulus [GPa]	14.4	14.4	14.4
Cross section's area [m ²]	0.640	0.375	0.500
Torsional moment of inertia [m ⁴]	0.0577	0.0017	0.0063
Second moment of inertia about local z axis [m ⁴]	0.0341	0.2035	0.0017
Second moment of inertia about local y axis [m ⁴]	0.0341	0.0177	0.2604

Table 2. Element properties.

The analyses were performed using OpenSees [8]. The numerical model consisted of beam elements representing the columns, the beams, the roof elements and the panels (their properties are shown in Table 2). In all analyses, the mean strength of steel and concrete was taken into account ([3], [5], [9]). In order to deal with the numerical inconsistencies that derive from localization problems of reinforced concrete frame elements appropriate regularization techniques were applied ([1], [6], [7]).

Following the precast concrete practice, pinned connections between beams and columns were adopted. Therefore, beams were simply supported and were modelled with elastic elements. For the columns, distributed plasticity model with 5 integration points was used for the plastic hinges and the moment-curvature relationship was idealized with a tri-linear curve connecting the points corresponding to the concrete cracking, the yield of the reinforcement and the concrete spalling. Plastic hinges could also form at the connections of the panels, which were modelled with the zero-length rotational spring mentioned above (Figure 3).

The roof elements were considered to behave elastically and were connected to the top of the beams with hinged connections (Figure 9a), either at a single point (Y-shape elements) or at two points (double-tee elements – Figure 9b).

Analyses were performed for two different behaviour laws concerning the roof-to-beam connections, namely: (a) fully elastic connections (non-yielding); (b) elastic – plastic connections (yielding). In the first case, forces of unrealistically large magnitude can develop in the roof-to-roof, roof-to-beam and beam-to-column connections for rigid diaphragms and strong ground motions, due to the kinematic constraints imposed to the deformation of the beams by the double-tee elements. For this reason, yielding roof-to-beam connections were considered in case (b), representing a “more realistic” situation. In this case, the resistance of the connections was determined taking under consideration the friction and the dowel action of the steel angle bolts, which was calculated according to Vintzeleou & Tassios formula ([11], [12]).

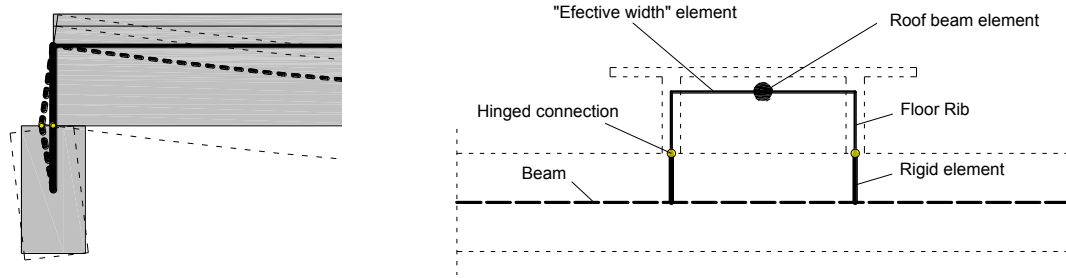


Figure 9. Roof-beam connections: (a) Schematic representation of the kinematic constraints; (b) Modelling of double-tee elements.

As mentioned above, the panels were modelled with five elastic beam elements and nonlinear zero-length rotational springs accounting for the overall nonlinear behaviour of the connections. For the determination of the moment – rotation constitutive law of these springs, pushover analyses were performed for the considered connections (Table 1) using the models of Figure 4. The derived capacity curves were transformed to bilinear curves, while sudden loss of strength was considered after the breakage of the bars. In order to capture the behaviour of the connection under cyclic loading, a hysteresis law was added. In Figure 10 such a hysteretic law for an indicative connection is depicted, while in Figure 11 the final idealised moment – rotation curves for the connections considered are shown.

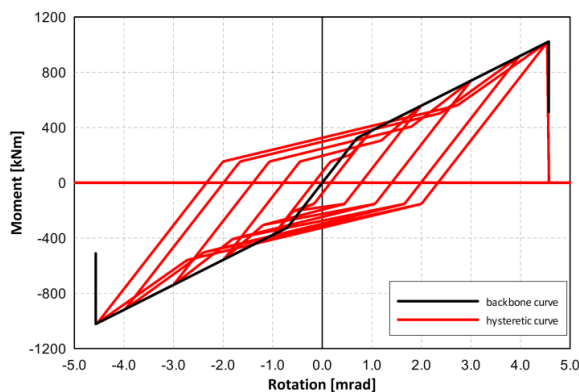


Figure 10. Hysteretic Moment – Rotation model of panel – beam connections made of 1Ø20 rebar and panels with four connections.

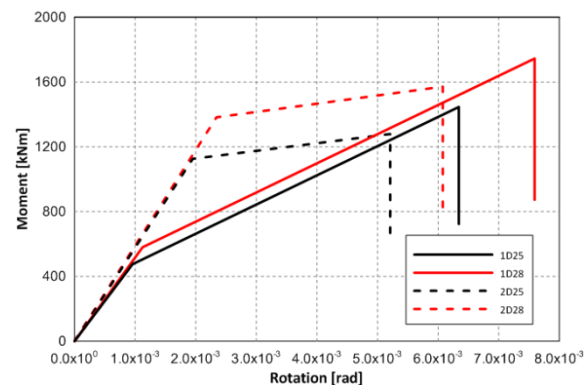


Figure 11. Idealised Moment – Rotation capacity curves of various panel – beam connections.

4 RESULTS OF THE NUMERICAL ANALYSES

4.1 Modal Analyses

Modal analyses were performed for buildings with integrated panels connected at three and four points and for buildings without panels; in the latter case, the panels contributed only with their mass (un-connected panels) while the structural system consisted of the bare frame only. Due to the large in-plane stiffness of the panels, the expected displacements of the buildings with panels were small and, for this reason, the columns were considered with their uncracked stiffness. Although this does not hold for the buildings without panels, the uncracked stiffness of the columns was also considered in that case in order to get comparable results.

As expected, the modes of vibration of the buildings with and without panels differ significantly. When the stiffness of the panels was neglected, the fundamental modes in both horizontal directions were translational with periods ranging from 0.90 to 1.19 sec for all types of

roof diaphragm. For the buildings with integrated panels, there were not clearly translational modes, while the effect of the diaphragmatic action was of major importance. The periods of the most important modes in each direction are given in Table 3. Indicative graphical representations of the most important mode are shown in Figure 12 for the building with deformable diaphragm.

No. of connections per panel	Diaphragm rigidity	Long direction		Short direction	
		Mode No.	Period [sec]	Mode No.	Period [sec]
4-point connections	Null	3	1.03	1	1.17
	Deformable	7	0.41	1	0.66
	Rigid	8	0.34	1	0.60
3-point connections	Null	3	1.03	1	1.17
	Deformable	7	0.43	1	0.68
	Rigid	6	0.40	1	0.64
Without panels	Null	3	1.13	1	1.19
	Deformable	2	0.90	1	0.93
	Rigid	2	0.99	1	1.03

Table 3. Periods of the important modes.

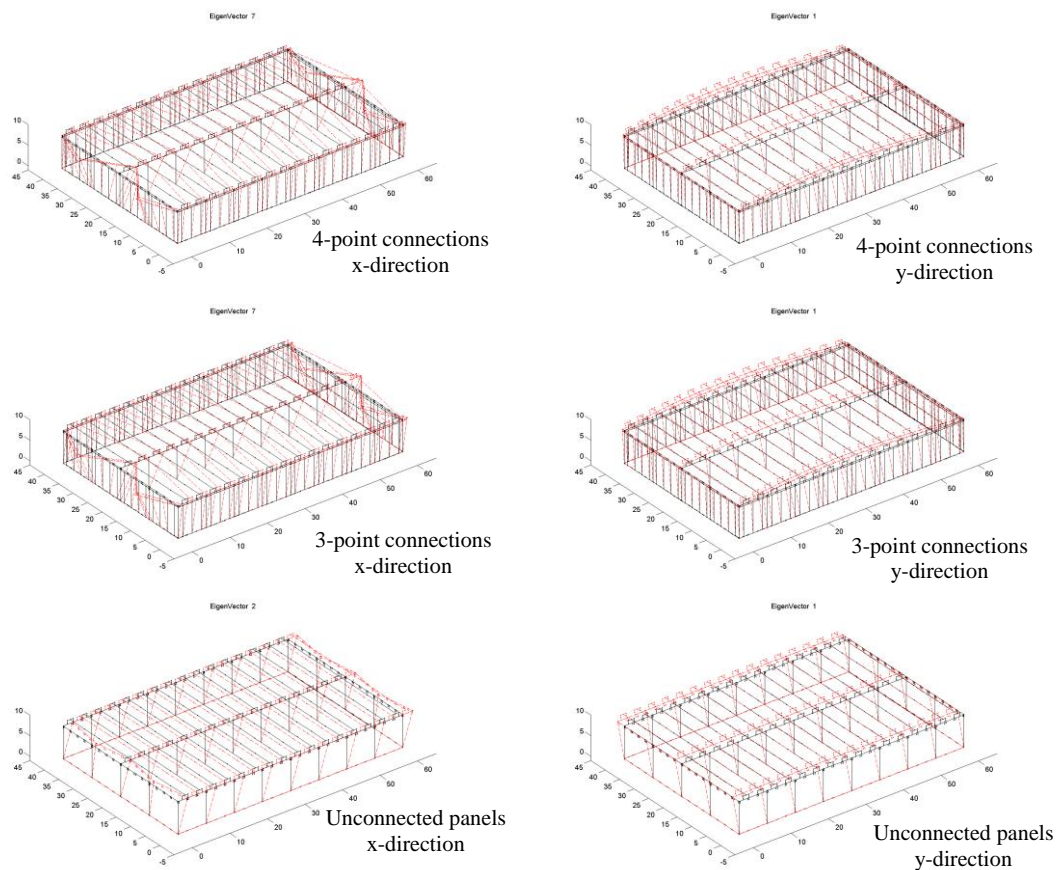


Figure 12. Most important mode of vibration for the building with deformable diaphragm.

4.2 Nonlinear Response History Analyses

For the nonlinear response history analyses (NLRHA), the modified Tolmezzo accelerogram (Figure 13a) was used. The record was modified to fit the EC8, type A response spec-

trum for soil category B (Figure 13b). Runs were performed for three levels of the peak ground acceleration (pga), namely: $pga = 0.18$ g (corresponding to 0.15 g for soil type A), $pga = 0.36$ g (corresponding to 0.30 g for soil type A) and $pga = 0.60$ g (corresponding to 0.50 g for soil type A).

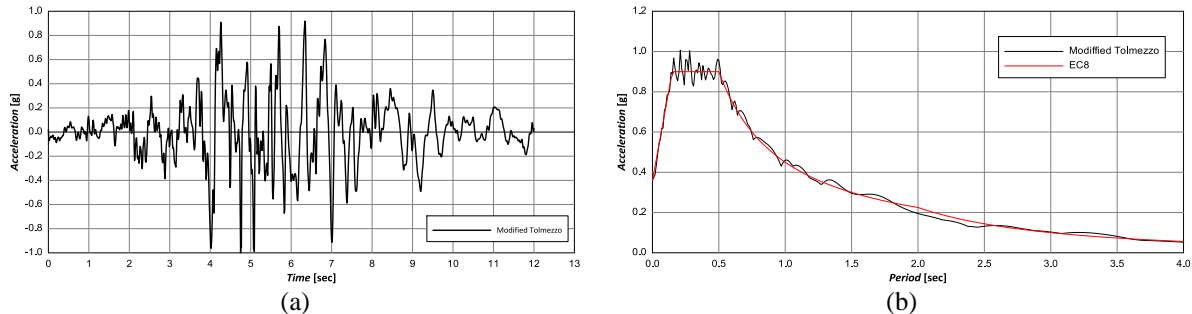


Figure 13. Modified Tolmezzo Accelerogram record used in the NLRHA: (a) Acceleration time history; (b) Response spectrum for $pga=0.36$ g and comparison with the EC8 spectrum.

The results show that the inelastic response observed in the structures was mainly due to the inelastic response of the columns and not of the panels, which behaved almost elastically. It is noted that, even for the rigid roof diaphragm, the drift of the internal columns and the columns located around the middle of the sides normal to the loading direction was considerably larger than the drift of the columns located at the external sides parallel to the loading direction (Table 4), which shows that there is significant in-plane deformation of the roof diaphragm leading to the yielding of the columns.

In general, it can be said that the response of structures with panels connected at four points showed similar characteristics with the response of structures with panels connected at three points.

Max drift [%]	Long direction			Short direction		
	0.18 g	0.36 g	0.60 g	0.18 g	0.36 g	0.60 g
External column in the side aligned with the direction of loading	0.09	0.16	0.33	0.10	0.30	0.56
External column in the side normal to the direction of loading	0.18	0.29	0.46	0.43	0.81	1.27
Internal column	0.18	0.29	0.46	0.31	0.64	1.06

Table 4. Maximum column drifts for the building with non-yielding roof-to-beam connections, rigid diaphragm and panels connected at four points.

When non-yielding roof-to-beam connections were considered, large forces developed in the roof-to-roof, roof-to-beam and beam-to-column connections, which in many cases exceeded their resistance. This phenomenon is attributed to the horizontal deflection of the longitudinal roof beams, which is restricted by the in-plane large stiffness of the double-tee elements. This is shown schematically in Figure 14: due to the deformation of the longitudinal beams, the displacements d_1 and d_2 at the two points where the double-tee roof elements are connected to the beams (at the bottom of their vertical ribs) are different from each other resulting in the distortion of the roof elements. It is evident that such large forces cannot develop in reality, as the roof-to-beam connections would yield or break leading to the relaxation of the internal forces induced to the structure.

Indeed, when yielding roof-to-beam connections were considered, the forces induced to beam-to-column connections were significantly reduced. However, large relative displace-

ments of the roof occurred in this case, which were affected by the diaphragmatic action of the roof and the intensity of the ground motion. The largest displacements were recorded for the flexible roof configuration and $pga = 0.60$ g, whereas no relative displacements generally occurred for $pga = 0.18$ g.

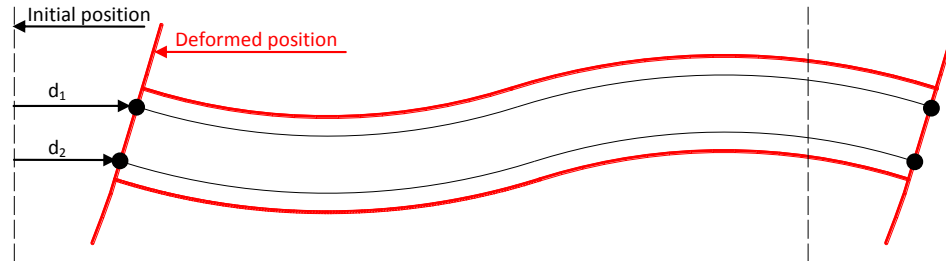


Figure 14. Deformation of roof double-tee elements during seismic loading.

5 CONCLUSIONS

The following conclusions can be drawn from the performed analyses:

- Buildings with integrated panel connections, resulting in the participation of the panels to the main structural system, are considerably stiffer than similar buildings with isostatic connections.
- The response of the structure with panels connected at four points shows in general similar characteristics with the one with panels connected at three points. However, there are differences in the values of the base shear and the top displacement.
- In systems with panels with integrated connections, the roof diaphragm has a profound effect on the way the forces are transmitted to the panels and the columns and, thus, affects significantly the overall seismic response. On the contrary, in buildings with panels free to move, the roof diaphragm rigidity does not affect the response of the structure.
- The nonlinear time history analyses performed for the modified Tolmezzo record show that much larger forces and displacements are induced to the internal columns than the external (façade) columns. The former behaved inelastically even for weak base excitations ($pga = 0.18$ g).
- The observed inelastic response is generally due to the inelastic response of the columns and not of the panels.
- In some connections, such as the roof-to-roof, roof-to-beam and beam-to-column, significant variation of the forces between connections located at different positions was observed. The larger forces developed at the roof-to-beam connections located close to the four corners of the building due to the horizontal deflection of the longitudinal beams during the seismic response, which cannot be easily accommodated by the double-tee roof elements due to their large in-plane stiffness. This phenomenon was significantly relaxed when yielding roof-to-beam connections were considered, but large relative roof displacements were observed in this case.

6 ACKNOWLEDGEMENTS

The research presented herein was conducted within the project “SAFECLADDING: Improved fastening systems of cladding wall panels of precast buildings in seismic zones”,

which was financed by the European Commission in the framework of the Seventh Framework Programme (FP7) under Grant Agreement number 314122. The first author wants to thank the Onassis Foundation for the financial support of his postgraduate studies at NTUA through Scholarship number GZI015.

REFERENCES

- [1] J. Coleman, E. Spacone, Localization issues in force-based frame elements. *Journal of Structural Engineering*, ASCE, **127**(11): 1257-1265, 2001.
- [2] Computers & Structures, Inc., *SAP2000 – Integrated Software for Structural Analysis & Design, Technical Reference Manual*
- [3] European Committee for Standardization (CEN), *Design of concrete structures – Part 1-1: General rules and rules for buildings*. Eurocode 2, EN 1992-1-1, 2004.
- [4] European Committee for Standardization (CEN), *Design of structures for earthquake resistance – Part 1: General rules, seismic actions and rules for buildings*. Eurocode 8, EN 1998-1, 2004.
- [5] European Committee for Standardization (CEN), *Design of structures for earthquake resistance – Part2: Bridges*. Eurocode 8, EN 1998-2, 2004.
- [6] International Federation for Structural Concrete (fib). *Practitioners' guide to finite element modelling of reinforced concrete structures*. Fib Bulletin 45, State-of-art report prepared by Task Group 4.4.
- [7] D.C. Kent, R. Park, Flexural Members with Confined Concrete. *Journal of the Structural Division*, ASCE, **97**(ST7): 1969-1990, 1971.
- [8] F. McKenna, G.L. Fenves, M. H. Scott, B. Jeremic, *Open System for Earthquake Engineering Simulation (OpenSees)*, Pacific Earthquake Engineering Research Center, University of California, Berkeley, CA., 2000.
- [9] T. Paulay, M.J.N. Priestley, *Seismic Design of Reinforced Concrete and Masonry Buildings*, John Wiley & Sons, New York, 1992.
- [10] SAFECLADDING, *Deliverable 3.3: Updates on numerical and experimental analyses of typical integrated arrangements*, FP7 GA No. 314122, 2015.
- [11] E.N. Vintzeleou, T.P. Tassios, Mechanics of load transfer along interfaces in reinforced concrete, prediction of shear force vs. shear displacement curves. *Studie de Reserche*, No. 7, Corpo di Perfezionamento per le Construzioni in Cemento Amato, Italcementi Societa per Azioni (S. p:A), Bergamo, Italy, pp. 121-161, 1985.
- [12] E.N. Vintzeleou, T.P. Tassios, Behavior of dowels under cyclic deformations. *American Concrete Institute (ACI)*, **84** (1): 18-30, 1987.